



**SPE 144167**

## **Translation of New Experimental Test Methods for the Evaluation and Design of Shaped Charge Perforators to Field Applications**

Hardesty, J., SPE, M.R.G. Bell, SPE, and N.G. Clark, SPE, GEODynamics, Inc., T. Zaleski, and S. Bhakta, INGRAIN, Inc.

Copyright 2011, Society of Petroleum Engineers

This paper was prepared for presentation at the 2011 SPE European Formation Damage Conference held in Noordwijk, The Netherlands, 7-10 June 2011.

This paper was selected for presentation by an SPE program committee following review of information contained in an abstract submitted by the author(s). Contents of the paper have not been reviewed by the Society of Petroleum Engineers and are subject to correction by the author(s). The material does not necessarily reflect any position of the Society of Petroleum Engineers, its officers, or members. Electronic reproduction, distribution, or storage of any part of this paper without the written consent of the Society of Petroleum Engineers is prohibited. Permission to reproduce in print is restricted to an abstract of not more than 300 words; illustrations may not be copied. The abstract must contain conspicuous acknowledgment of SPE copyright.

### **Abstract**

Perforation performance evaluation has come under scrutiny in several recent publications. For most shaped charge perforators sold, performance is evaluated in cement targets, from which downhole performance is extrapolated. This method has been shown to generally over-predict downhole performance, with broad implications for perforating systems and shaped charge design, and well completion design.

Advanced test methodologies are an order of magnitude more complex than the simplified cement penetration tests. This paper details a set of experimental shaped charge development programs with specific geometry and/or flow performance requirements and examples of their corresponding field performance. Tests have been performed with full simulation of single shot perforation, and simplified perforating simulations into stressed rock. Results are reported for shale, sandstone, and high permeability sandstone targets. Designs tested include both conventional and reactive shaped charges.

In one example from 2008-2009, CNX completed fourteen wells using both conventional and reactive perforating systems to evaluate any impact on completion performance. Stimulation and production data have been analyzed for 81 stimulation stages. When comparing wells perforated with reactive shaped charges to conventionally perforated offsets, a reduction in breakdown pressure gradient of between 13% and 29% is observed. Subsequent treating pressures are reduced by 6% to 15%. The wells perforated with reactive shaped charges have also exhibited significantly slower productivity decline over the first nine months.

In addition, near-perforation permeability has been mapped using advanced digital imaging techniques. This allows the grain structure and permeability distribution of a perforated rock target to be accurately measured as a function of radial distance away from the perforation wall and longitudinal position along the perforation tunnel. The paper describes important improvements in our understanding of perforation damage distribution, and provides techniques for use in conjunction with API RP 19B Section 2 and 4 tests to design perforating shaped charges and systems.

### **Background and Introduction**

Perforation performance evaluation has become a crucial issue in the modern perforating industry. Several recent papers have discussed the insufficiency of API RP 19B Section 1 cement penetration tests to accurately predict downhole performance. (Behrmann et al, 2009, Gladkikh et al, 2009, Harvey et al, 2010) The tunnels created in cement target are long and narrow, and shaped charges have undergone extensive optimization to create penetrations in these cement targets up to 63 inches in length. (API Registered 19B Section 1 data) The industry standard models used to predict the performance of perforating systems downhole conditions are based on performance in cement targets are essentially linear relationships based on rock strength and stress ratios. These models were established with perforating systems which penetrated less than half of the modern cement maximum penetration distance. (Ott et al, 1994). Due to this, most industry standard models significantly over predict downhole penetrations, and have done so for years. Laboratory studies suggest that downhole perforation tunnels are often only one half to one third of the predicted perforation tunnel length.

In addition, penetration length is only one aspect of total perforation tunnel geometry. The primary purpose of the perforation tunnel is to provide a connection between the cased well and the surrounding formation. In some applications this connection is the sole means of transferring fluid into the wellbore, in others, this connection is the vehicle for stimulation treatment. In both cases, the perforation diameter, casing entry hole, perforation wall condition, permeability reduction, and tip condition may play a role in the final performance of the well and/or in the ease of applying the stimulation treatment. None of these aspects of perforation may be predicted from results in cement targets (Bell et al, 2008).

Perforation geometry may often take a form where a significant length of the perforation tunnel is filled with compacted rock around a compacted metal core – which reduces the effective length of the perforation tunnel for many applications. Industry standard penetration models predict open tunnel tips which reach out to multiples of the original well borehole diameter. With the reductions indicated by laboratory testing factored in, these penetration lengths will typically only reach a distance equivalent to ½ to 1-1/2 times the original borehole diameter. In this case, the perforation tunnel will be a near wellbore event, and will interact with the near wellbore damage rather than with the undamaged formation as is often assumed. (Gladkikh et al, 2009)

The over prediction of downhole perforation performance and the neglect of the actual perforation geometry have significant implications for perforating strategies, the well completion process, and for the perforating industry. Perforation strategies may be decided on a cost basis, since all solutions appear to provide sufficient penetration for the application. Restrictions that preclude the use of perforation systems correctly sized for the casing may be built into the well completion, based on the assumption that the sub sized systems provide sufficient performance. Finally, with inflated performance predictions negating the difference between precision perforating products and commodity products, the perforating market has moved to preclude development which relies on more expensive testing, higher precision manufacturing, or higher quality materials. Bespoke engineered perforating solutions are rarely applied.

A major use of perforation performance data over the past decades has been the application to well inflow models. In addition to an overestimated penetration length and exaggerated clear tunnel, these models often use a simplification of the permeability distribution around the perforation tunnel of a constant thickness, constant reduced value permeability. The results presented in this paper show a much more complex permeability distribution, and also shows improved side wall permeability for most regions of perforations created with reactive shaped charges in Berea Sandstone. The updated permeability distribution observed in these tests may affect any conclusions derived from models based on the simplified permeability distribution, including acidizing, injection, or inflow models.

Advanced perforation evaluation technology has been available for the last 30 years, but is still today in the process of being properly utilized. The most versatile of these technologies is the single shot perforation test into cylindrical stressed rock targets, commonly referred to as an API Recommended Practice 19B Section 2 or Section 4 test. In the United States today, there are three major service companies and one independent manufacturer of perforating equipment which have the capability of performing perforation tests into cylindrical stressed rock targets. Two of these four facilities are less than 5 years old. These testing methodologies are not yet perfect simulations of the downhole environment, substituting uniform rock of limited sample sizes with imperfect boundary conditions and stress application for semi-infinite, formation rock with near wellbore effects. Nevertheless, these tools may be used in conjunction with specific development criteria to develop perforation products which translate well to field applications, although always with some degree of uncertainty.

This work details the application of these tests in conjunction with specific design criteria, which results in improved perforating systems. Three sets of laboratory data are presented, showing flow performance and perforation geometry produced from stressed rock cylindrical targets. Initial data as a result of underbalance in Berea Sandstone is presented, along with geometry performance in Mancos Shale. Additionally, a new reactive shaped charge design is demonstrated to have performance improvement in high permeability sandstone. Finally, a field study conducted in Chattanooga Shale demonstrates the performance translation from the laboratory to the field.

## Experimental Procedure

The Perforation Flow Cell at GEODynamics provides a tool for perforation geometry evaluation and basic flow evaluation, as shown in Figure 1. Various initial perforation conditions can be applied to the target sample, which allows evaluation of subtle design variations that affect cleanup and other tunnel geometry. Perforation flow evaluation provides translation between tunnel geometry and well production results. The facility accommodates perforating tests at up to 10,000 psi confining and 5,000 psi wellbore and pore pressures, with up to 5 inch diameter targets. Flow testing, both pre-shot and post shot, is conducted with back pressure to minimize pressure fluctuation effects.

Three series of tests were conducted, one each with Berea Sandstone, Castlegate Sandstone, and Mancos Shale. With the exception of the shale targets, each of the 5.0 inch diameter by 18 inch long targets was first dried to constant weight, and then vacuum saturated with odorless mineral spirits (OMS). The target was placed in the core fixture, and the axial permeability was measured at 5000 psi overburden and 1000 psi back pressure. Following this, the shaped charge was loaded in a simulated gun inside the wellbore fixture, and pressures were raised to those desired. In all three test series, overburden was 8000 psi, and pore pressure was 4000 psi. Wellbore pressure was varied in order to create the desired under or overbalance condition.

The shaped charge was detonated, and the pressures were allowed to equalize. The gun volume was similar to that found in production guns per shaped charge, and sized with the rest of the system to generate minimal dynamic under or overbalance. The resulting perforation was tested for production flow performance at a standard set of flow rates. Flow rate, temperature, and pressure drop were measured, and nondimensionalized by the initial flow performance of the target to provide a standard Production Ratio (PR). The perforations were then measured, and the targets split. None of the tunnels pictured were altered or scrubbed to remove crushed material.

## Presentation of Results

The baseline tests for all studies were conducted with a 15.0 gram HMX shaped charge which has a registered API RP 19B Section 1 cement penetration of 35.1 inches. In the first study, this shaped charge was used to perforate Berea Sandstone targets that are 5.0 inches in diameter and 18 inches long. This set of Berea Sandstone has typical properties of 100-150 mD permeability, 19% porosity, and 7000 psi uniaxial compressive strength. Four tests were conducted with the conventional shaped charge, in which the initial wellbore pressure was varied in order to demonstrate the sensitivity of the produced perforation geometry to surge flow clean up. The typical penetration into these targets was 8-9 inches, as shown in Table 1. This penetration was relatively insensitive to the initial balance condition. Flow performance, as measured by PR, varied with initial balance condition, as shown in Table 1 and Figure 2. This is primarily due to the change in geometry as the overbalance condition inhibits surge flow clean up and allows the creation of the perforation geometry structure pictured in Figure 3. This is typical of conventional powdered metal lined perforators formed without sufficient surge flow to break up the competent structures. In the conventional perforation event, the perforator jet penetrates into the rock, piercing and pushing aside the original rock structure. When the jet material is no longer moving fast enough to penetrate the target, it begins to stack up acting as the keystone of an arch to hold all of the crushed material in place. In laboratory flow testing, this structure is rarely removable with normal flow rates.

The reactive shaped charge for this application was designed using stressed rock testing and development facilities to create perforations with equivalent penetration as the conventional shaped charge in Berea Sandstone targets and in generic 10,000 psi sandstone targets, while demonstrating improved perforation geometry, including tunnel diameter, clean up, side wall permeability, and tip geometry. The reactive component aids in this role by applying radial mechanical and thermal energy during the penetration event which helps to prevent the formation of the wedged target pack, remove the packed metal core, and also to cause clean up and fractures at the tip of the perforation. The geometry produced by this design strategy can be observed in Figure 4. The flow performance of the reactive shaped charge is shown to be 55 to 76% superior to the conventional shaped charge at every balance condition. Furthermore, in these tests, the reactive shaped charge at 1000 psi overbalance condition performed equivalently to the conventional shaped charge with 500 psi underbalance. With slight underbalance, the reactive perforation tunnel flow performance surpasses the performance of the original full face axial flow through the unperforated core.

The target rock in the second study was Castlegate Sandstone, which has typical permeability of between 700 and 900 mD, 20-21% porosity, and 5000 psi uniaxial compressive strength or less. The same conventional shaped charge was used as the baseline; however the reactive shaped charge was redesigned in order to produce the best possible geometry in these targets, effectively becoming a different product. Production ratios for the conventional shaped charges were significantly higher, as these shaped charges performed well in the soft targets, creating deeper tunnels combined with adequate clean up. The optimized reactive shaped charge demonstrated superior flow performance, ranging from 6% to 59% improvement in flow performance, and even providing a PR of 0.92 at overbalanced conditions. These results are shown in Figure 5 and Table 2. Comparing the geometry at balanced conditions in Figures 6 and 7, the conventional shaped charge produced significantly deeper tunnels; however the reactive shaped charge produced cleaner tunnels with better side wall conditions.

The third laboratory study was conducted in Mancos Shale. This shale typically has low porosity and permeability, so flow testing was not conducted, and perforation geometry results are only compared. Tests were conducted at the same conditions as the other two studies, at 500 psi underbalance, balanced conditions, and at 500 psi overbalance. These results are reported in Table 3. As expected, the open tunnel was not sensitive to the pre-shot wellbore pressure, although it was surprising to see a slight decrease in total penetration for both shaped charges with increasing underbalance. The penetrations were similar, with the conventional shaped charges having a slight increase in total penetration at every condition. The reactive shaped charges did provide significantly increased open tunnel lengths, ranging from 140% to 309% improvement. The perforation tunnels are also significantly larger in diameter and more structurally sound, as shown in Table 3 and in Figures 8 and 9. The reactive shaped charge tested in this study was identical to the shaped charge tested in study 1, and therefore not optimized for this target.

In the field, this laboratory performance has been shown to translate positively. Figures 10 and 11 show average results from fourteen wells completed by CNX between May 2008 and October 2009 in the Chattanooga Shale properties in Northern Tennessee. The CNX development features horizontal wells at depths between 2,300 and 4,600 feet, completed with 4-9 fracture stimulations. Treatment sizes vary from 15,000 to 30,000 gallons and 50,000 to 100,000 pounds of proppant, typically assisted by 70-quality foam. The wells were completed with both reactive and conventional perforating systems. Stimulation and production data have been analyzed for 81 stimulation stages. When comparing wells perforated with reactive shaped charges to conventionally perforated offsets, a reduction in breakdown pressure gradient of between 13% and 29% is observed. Subsequent treating pressures are reduced by 6% to 15%. Productivity decline data in Figure 12 indicates a reduction in productivity decline over the first nine months. This may be indicative of improved fracture placement and/or superior connectivity between wellbore and fracture.

Figures 13 and 14 are CT scans of perforated stressed rock Berea sandstone that has been imaged using INGRAIN's digital rock physics lab. The depicted slices correspond to locations for subsamples which are sectioned in 2 mm increments and scanned at a high resolution to enable computation of the permeability distribution longitudinally along and radially away from the tunnel wall. For each perforation tunnel there are a total of 84 permeability calculations taken to map the permeability distribution. Figure 15 shows the permeability map of a conventional perforation tunnel, with permeabilities less than 50 mD at the tunnel wall which gradually increase to far field 100 mD. Positions closer to the tip of the tunnel have higher permeabilities than those near the tunnel entrance. Figure 16 is the permeability map of the reactive perforation tunnel. Permeability values are significantly increased, with a much larger proportion of samples above the 100 mD line. As the distance from tunnel increases for sample 3 and 4, permeability exceeds the unaltered rock permeability, possibly as a result of the numerous fractures generated at the tip of the perforation tunnel. Figure 17 is a graph of the percentage increase in similar locations from the conventional perforation to the reactive perforation. Although there is some local decrease in permeability at subsample 2, most of the reactive perforation tunnel has significantly higher permeability, especially at the tip.

## Conclusions

Perforating system design and technology is an important part of many completion applications. Overreliance upon misleading penetration models has caused lost productivity. The interaction of perforation geometry with near wellbore conditions is relevant to well performance for many completions.

Shaped charge design methodology based upon the creation of advantageous geometry to improve flow performance in sandstone of 10 – 200 mD, and utilizing reactive technology has been demonstrated to be effective in the laboratory and in the field. Shaped charges based upon this design methodology have significantly improved performance with little or no surge flow cleanup caused by underbalance.

This design methodology combined with reactive perforating has been successfully applied in the laboratory to produce perforating flow performance improvement in balanced and overbalanced situations in sandstone with permeability in the range of 800 mD.

Shaped charges designed for the 10 – 200 mD formations demonstrate geometry improvement in laboratory experiments with Mancos Shale. This laboratory performance improvement translates to field performance improvement in shale fields such as the Chattanooga Shale, reducing fracture breakdown pressure, fracture treatment pressure, and may also reduce long term productivity decline. This confirms and reinforces previously reported field improvements. (Bell et al, 2008, 2009, Qayyum et al, 2009)

It is likely that future work could develop a perforating system which is better suited for shale fields.

In laboratory experiments, the use of advanced imaging techniques has demonstrated that reactive shaped charges produce improved permeability in the side walls of perforations created in Berea Sandstone compared to the permeability in the side wall of perforations produced with conventional shaped charges in similar targets.

## Acknowledgments

The authors would like to thank Sean Brake and CNX Gas Company, LLC for the generous sharing of their field experience with reactive perforators. The authors would also like to thank Chris Pool and David Newcomb for all of their efforts on behalf of these studies.

## References

- Behrmann, L. B. Grove, SPE, I. Walton, SPE, L. Zhan, SPE, C. Graham, SPE, D. Atwood, SPE, and J. Harvey, SPE, Schlumberger, "A Survey of Industry Models for Perforator Performance; Suggestions for Improvements" SPE 125020-MS SPE Annual Technical Conference and Exhibition, 4-7 October 2009, New Orleans, Louisiana.
- Bell, M.R.G., J. Hardesty, and N.G. Clark, GEODynamics Inc. "A New Technique for the Development and Quality Control of Flow-Optimized Shaped Charges" SPE 19331-MS Offshore Technology Conference, 5-8 May 2008, Houston, Texas, USA
- Bell, M.R.G., SPE, GEODynamics Inc., and D.A. Cuthill, SPE, Weatherford Canada Partnership. "Next Generation Perforating System Enhances the Testing and Treatment of Fracture-Stimulated Wells in Canada" SPE 116226-MS SPE Annual Technical Conference and Exhibition, 21-24 September 2008, Denver, Colorado, USA
- Bell, M.R.G., Hardesty, J.T., Clark, N.G.: "Reactive Perforating: Conventional and Unconventional Applications, Learnings and Opportunities", SPE 122174, SPE European Formation Damage Conference, Netherlands, 27-29 May 2009.
- Gladkikh, M. and W.B. Harvey, Baker Hughes; P.M. Halleck, The Pennsylvania State University, "Predicting Depth of Penetration of Downhole Perforators", SPE 124783-MS SPE Annual Technical Conference and Exhibition, 4-7 October 2009, New Orleans, Louisiana.
- Gladkikh, M., Brian LeCompte, William Harvey, Alexander Makarov, Yuriy Antonov, Baker Hughes; Phillip M. Halleck, Penn State University, "Combining the Prediction of Penetration Depth of Downhole Perforators with the Depth of Invasion", SPE 122319-MS 8th European Formation Damage Conference, 27-29 May 2009, Scheveningen, The Netherlands.
- Harvey, J., SPE, B. Grove, SPE, and L. Zhan, SPE, Schlumberger, and L. Behrmann, SPE, Consultant, "New Predictive Model of Penetration Depth for Oilwell Perforating Shaped Charges" SPE 127920-MS SPE International Symposium and Exhibition on Formation Damage Control, 10-12 February 2010, Lafayette, Louisiana, USA
- Ott, R.E., Mobil E&P U.S. Inc.; Bell, W.T., Consultant; Schlumberger Wireline and Testing; Golian, T.G., "Simple Method Predicts Downhole Shaped-Charge Gun Performance" SPE 27424-PA SPE Production & Facilities, Volume 9, Number 3 August 1994 pp. 171-178.
- Qayyum, T., SPE, K. Khattak, SPE, I. Qureshi, SPE, and T. Aizad, SPE, Eastern Testing Services, and S. Hameed, SPE, and S. Akhtar, SPE, Dewan Petroleum Ltd., "Successful Introduction of Next Generation - Reactive Liner Perforating Technology in Pakistan" SPE 125901-MS SPE/IADC Middle East Drilling Technology Conference & Exhibition, 26-28 October 2009, Manama, Bahrain

Figures and Tables

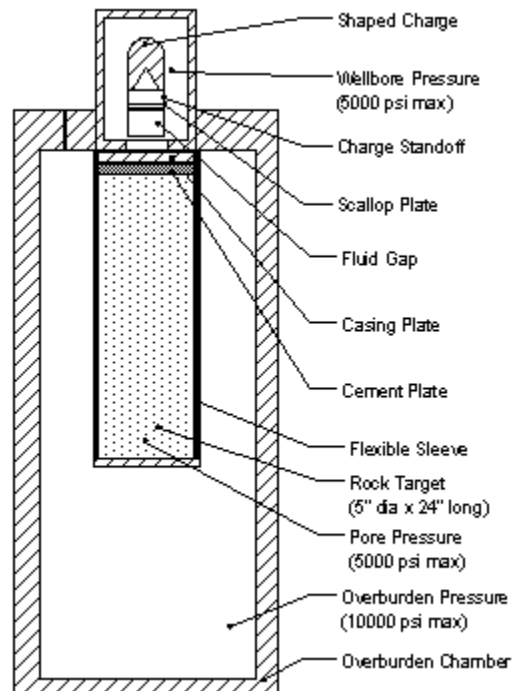


Figure 1: GEODynamics Perforation Flow Cell Schematic

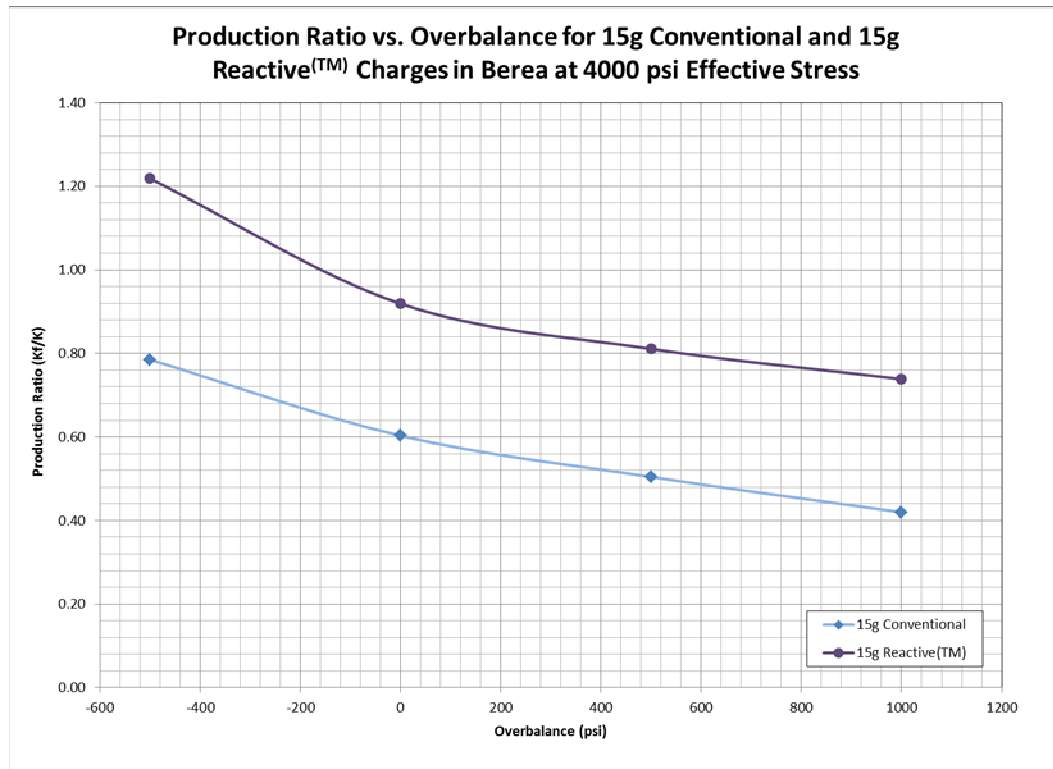


Figure 2: Flow Performance of Conventional and Reactive™ Charges in Berea Sandstone

Charge	Balance (psi)	Pen. (in)	Permeability (mD)	Post S Flow (mD)	PR -	Flow Imp. -
2715 Conventional	1000	9.20	142	60	0.42	
2715 Reactive	1000	8.20	143	106	0.74	76%
2715 Conventional	500	6.20	106	53	0.50	
2715 Reactive	500	8.60	106	86	0.81	61%
2715 Conventional	0	8.85	130	79	0.60	
2715 Reactive	0	9.05	111	102	0.92	52%
2715 Conventional	-500	9.05	113	88	0.79	
2715 Reactive	-500	9.10	140	170	1.22	55%

Table 1: Performance Comparison of 15g Conventional and Reactive™ Charges in Berea Sandstone

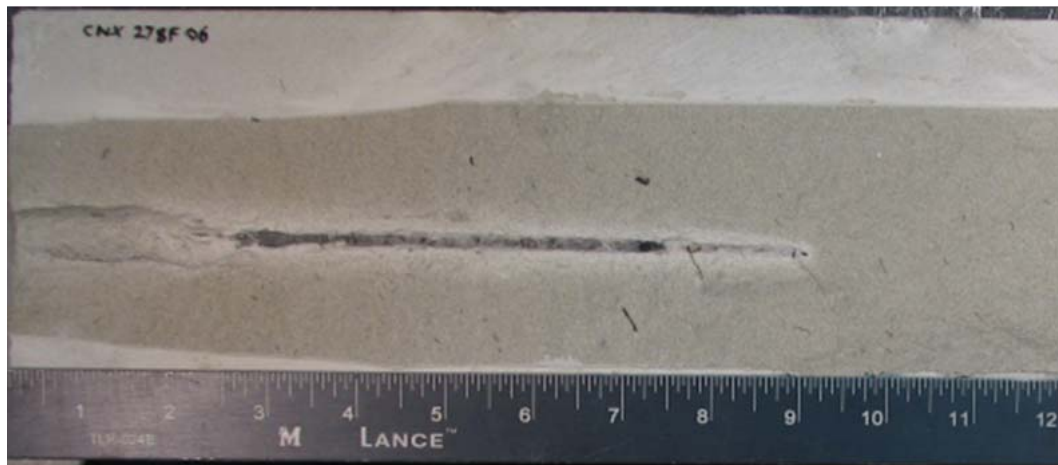


Figure 3: Conventional 15g Charge at Overbalance Conditions in Berea Sandstone



Figure 4: Reactive 15g Charge at Overbalance Conditions in Berea Sandstone.

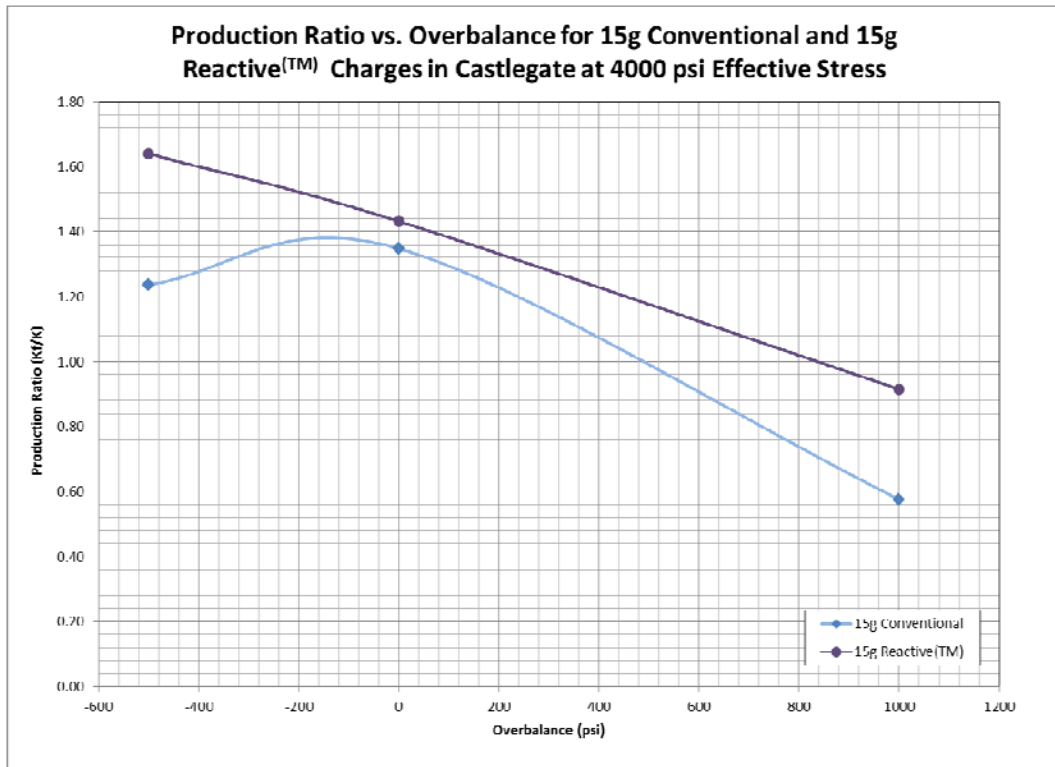


Figure 5: Flow Performance of Conventional and Reactive<sup>TM</sup> Charges in Castlegate Sandstone

Charge	Balance (psi)	Pen. (in)	Permeability (mD)	Post S Flow (mD)	PR	Flow Imp.
15g Conventional	1000	12.40	750	432	0.58	
15g Reactive	1000	10.90	830	760	0.92	59%
15g Conventional	0	13.70	660	890	1.35	
15g Reactive	0	10.90	870	1246	1.43	6%
15g Conventional	-500	11.67	776	960	1.24	
15g Reactive	-500	9.55	899	1476	1.64	33%

Table 2: Performance Comparison of Conventional and Reactive<sup>TM</sup> Charges in Castlegate Sandstone

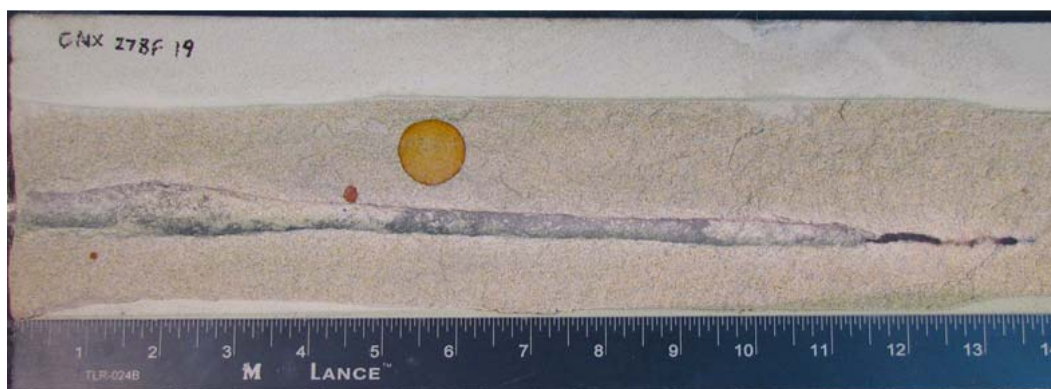


Figure 6: Conventional 15g Charge in Castlegate at Balanced Condition

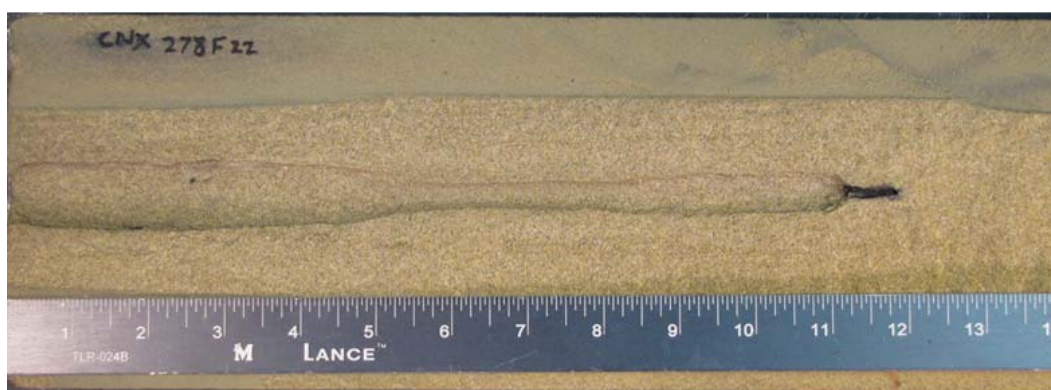


Figure 7: Reactive™ 15g Charge in Castlegate at Balanced Condition

Charge	Balance (psi)	Open Tunnel(in)	Pen (in)	% Clear (%)	Max Tunnel Dia (in)	Tunnel @ 90% (in)	Tunnel Imprvmt
15g Conventional	500 Under	2.55	6.5	39%	0.18	0.17	
15g Reactive™	500 Under	6.10	6.4	95%	0.32	0.21	139%
15g Conventional	Balanced	1.70	7.8	22%	0.27	0.16	
15g Reactive™	Balanced	6.95	7	99%	0.3	0.12	309%
15g Conventional	500 Over	2.60	8.1	32%	0.23	0.09	
15g Reactive™	500 Over	6.25	7.2	87%	0.29	0.19	140%

Table 3: Performance Comparison of 15g Conventional and Reactive™ Charges in Mancos Shale



Figure 8: Conventional 15g Charge in Mancos Shale



Figure 9: Reactive™ 15g Charge in Mancos Shale

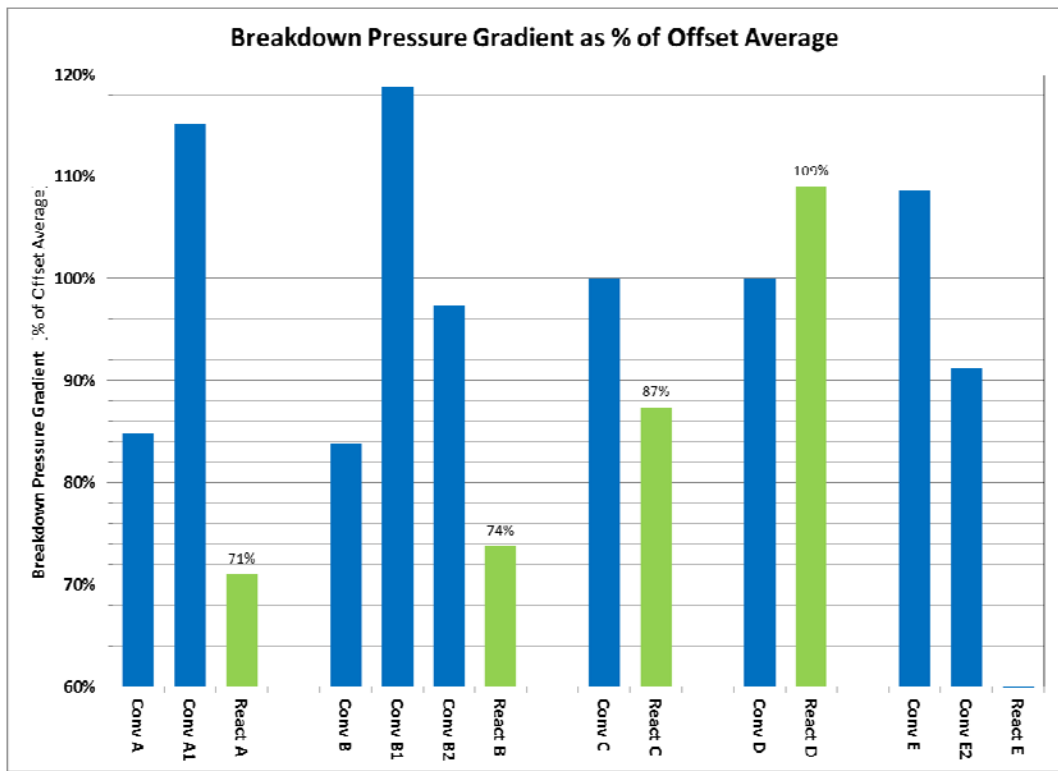


Figure 10: Chattanooga Shale Breakdown Pressure Gradient as Percent of Offset Average

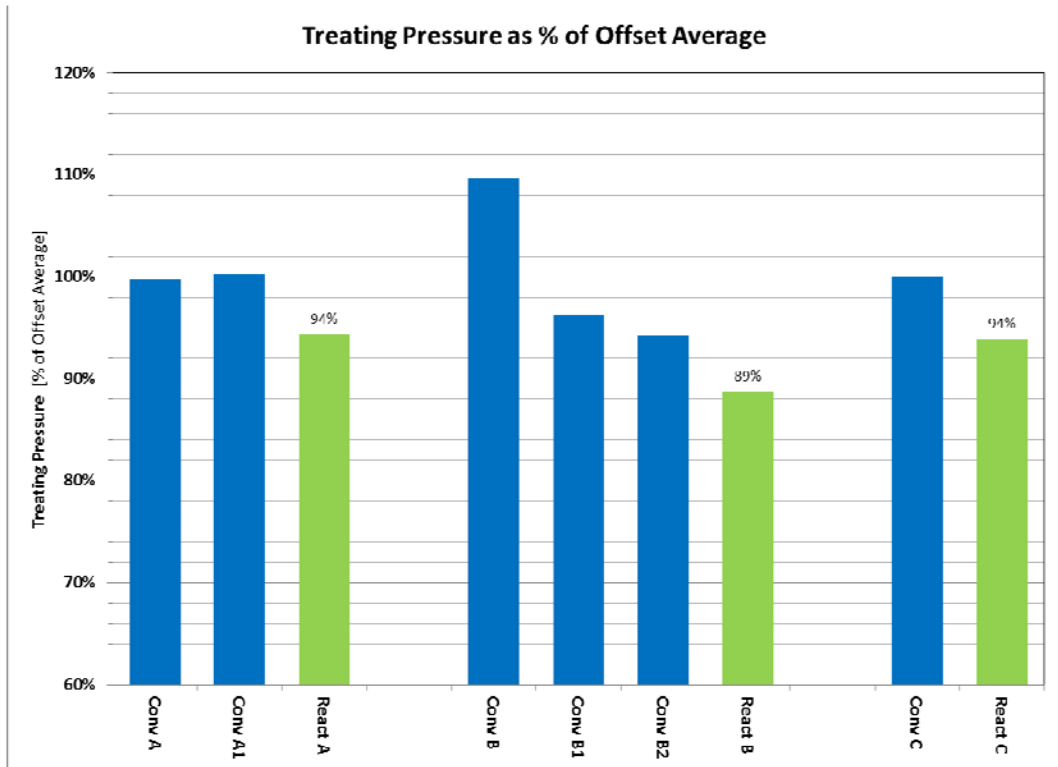


Figure 11: Chattanooga Shale Treating Pressure as Percent of Offset Average

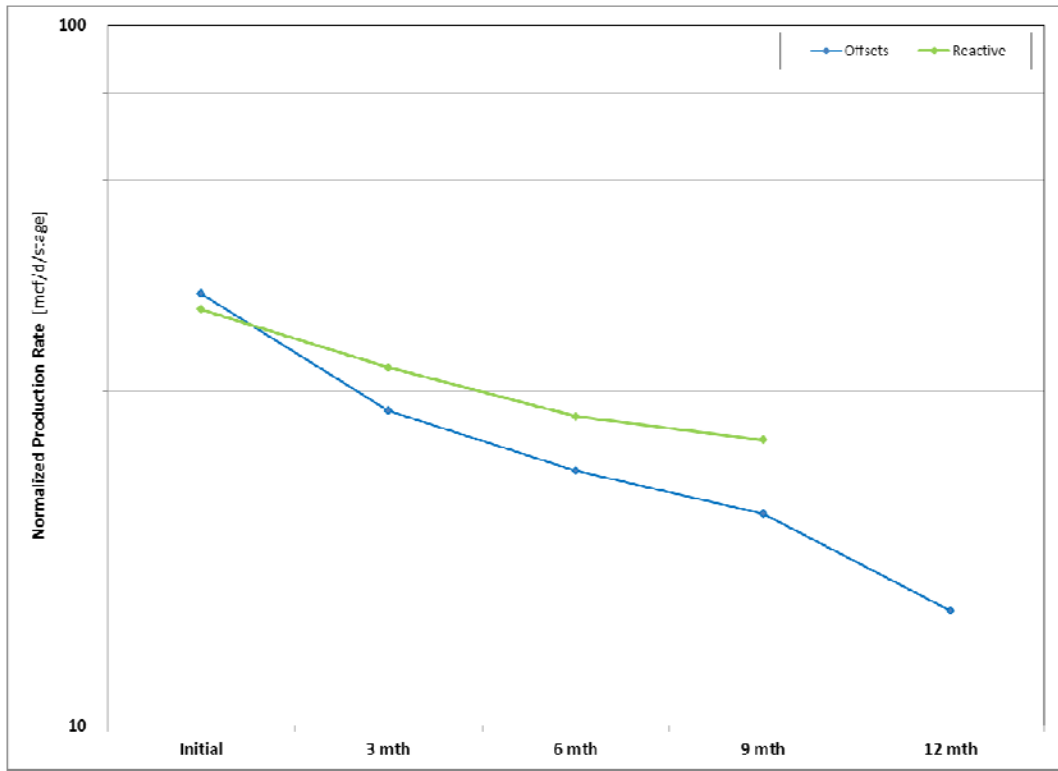


Figure 12: Chattanooga Shale Early Time Average Normalized Productivity Decline

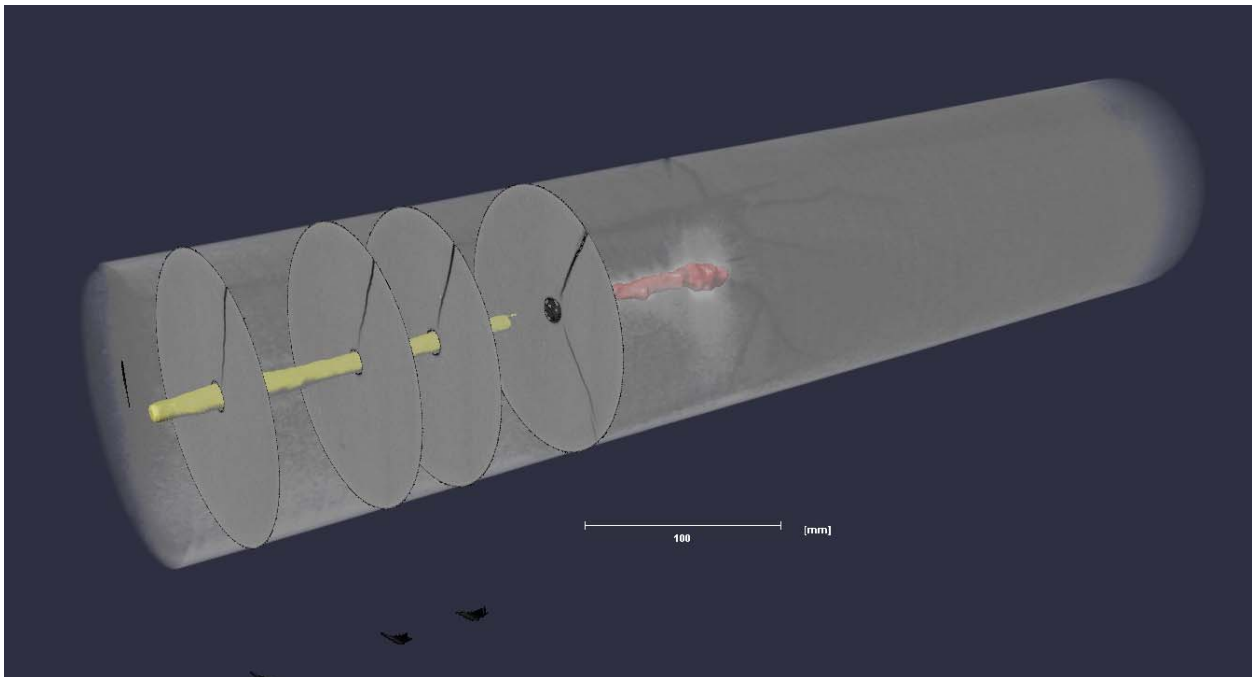


Figure 13: Conventional Charge Scan and Sample Locations

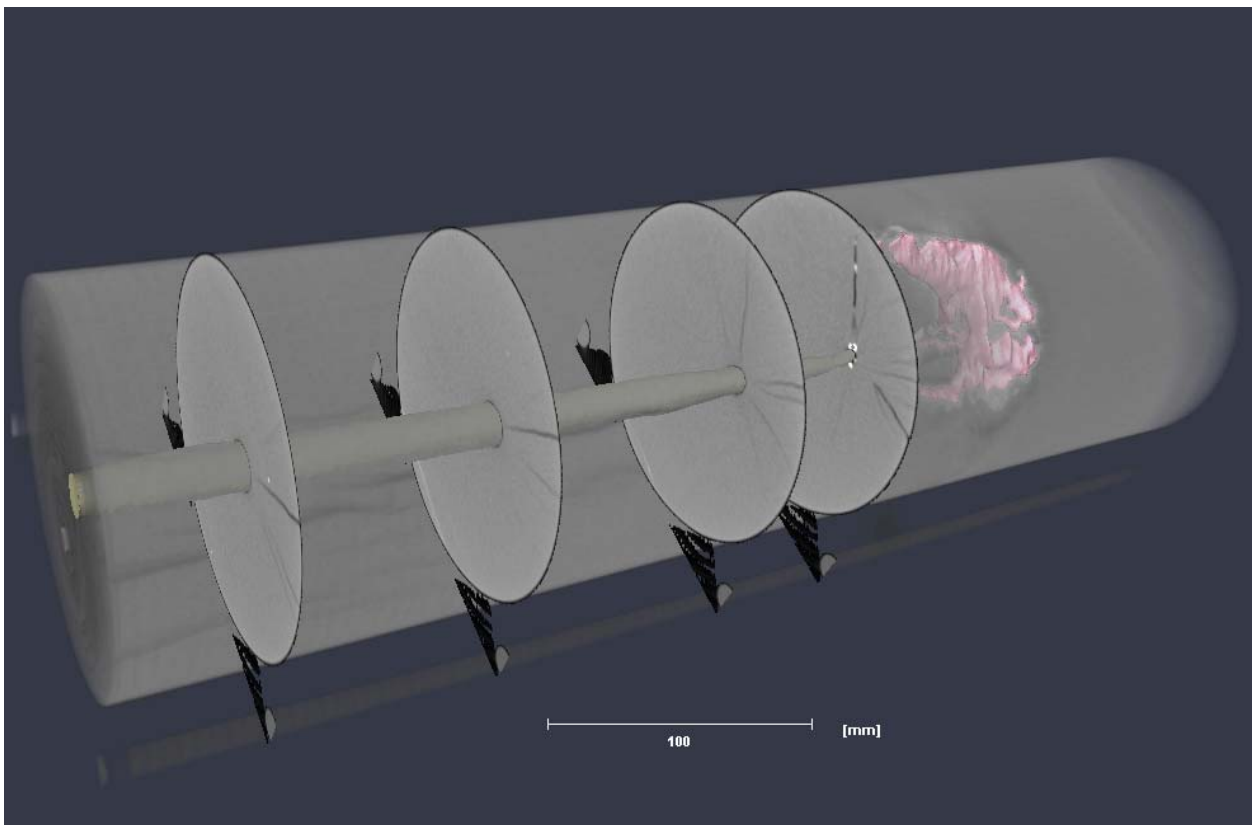


Figure 14: Reactive Charge Scan and Sample Locations

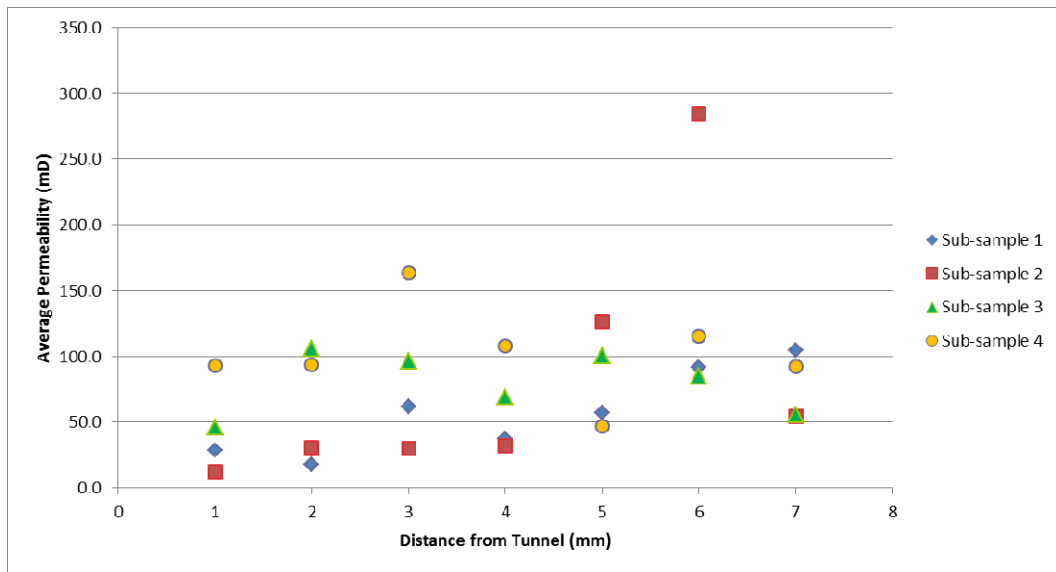


Figure 15: Average Permeability Distribution of Conventional Perforation Tunnel

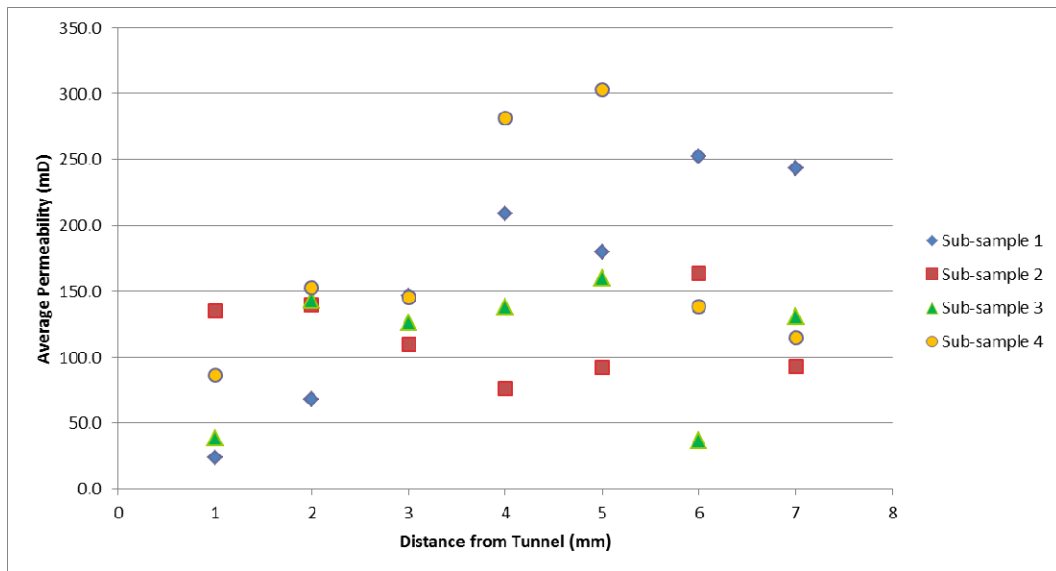


Figure 16: Average Permeability Distribution of Reactive Perforation Tunnel

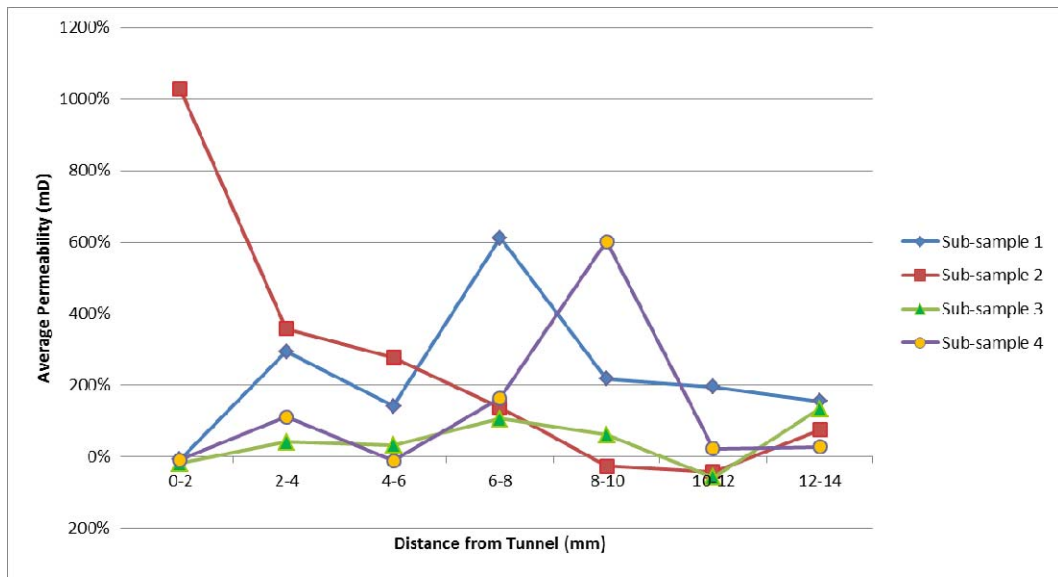


Figure 17: Average Permeability Improvement of Reactive Charge compared to Conventional Charge